

Lawrence Berkeley National Laboratory

Recent Work

Title

CURRENT DISTRIBUTION ON A ROTATING RING-DISK ELECTRODE BELOW THE LIMITING CURRENT

Permalink

<https://escholarship.org/uc/item/2dk7s4tt>

Author

Pierini, Peter

Publication Date

1976-08-01

0 0 0 0 4 0 0 4 3 0 5

Submitted to Journal of Electrochemical Society

LBL-5492
Preprint C. |

CURRENT DISTRIBUTION ON A ROTATING RING-DISK ELECTRODE BELOW THE LIMITING CURRENT

Peter Pierini and John Newman

RECEIVED
LIBRARY
BERKELEY LABORATORY

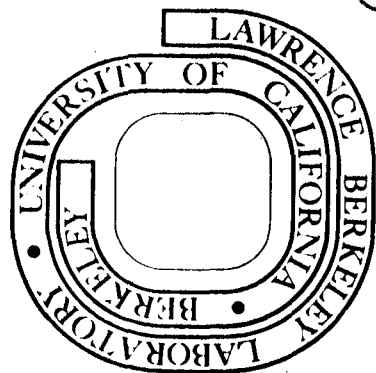
August 1976

SEP 1 1976

LIBRARY AND
DOCUMENTS SECTION

Prepared for the U. S. Energy Research and Development Administration under Contract W-7405-ENG-48

For Reference
Not to be taken from this room



LBL-5492
C. |

DISCLAIMER

This document was prepared as an account of work sponsored by the United States Government. While this document is believed to contain correct information, neither the United States Government nor any agency thereof, nor the Regents of the University of California, nor any of their employees, makes any warranty, express or implied, or assumes any legal responsibility for the accuracy, completeness, or usefulness of any information, apparatus, product, or process disclosed, or represents that its use would not infringe privately owned rights. Reference herein to any specific commercial product, process, or service by its trade name, trademark, manufacturer, or otherwise, does not necessarily constitute or imply its endorsement, recommendation, or favoring by the United States Government or any agency thereof, or the Regents of the University of California. The views and opinions of authors expressed herein do not necessarily state or reflect those of the United States Government or any agency thereof or the Regents of the University of California.

Current Distribution on a Rotating Ring-Disk
Electrode below the Limiting Current

Peter Pierini and John Newman^{*}

Materials and Molecular Research Division, Lawrence Berkeley Laboratory,
and Department of Chemical Engineering, University of California,
Berkeley, California 94720

August, 1976

Abstract

Ring-disk electrodes have been used in the literature to simulate experimentally the nonuniform current distribution across a rotating disk electrode operated at a fraction of the limiting current. The analogy of a sectioned disk to a ring-disk electrode is difficult to substantiate since both the limiting current and primary current distributions are radically different. Thus a detailed knowledge of the distribution of current and concentrations is developed to compare rationally the differences in nonuniformity for the ring-disk and disk electrodes. Integral measures of the degree of departure from the limiting current and primary current distributions are developed and related to the measurement of throwing power.

^{*} Electrochemical Society Active Member

Key Words: sectioned disk, throwing power, potential distribution

Introduction

The ring-disk electrode system is one of the most convenient arrangements of two working electrodes in a common cell. The concentric, rotating electrode structure is relatively easy to fabricate and is available commercially. The device has drawn attention recently, as both the object of theoretical analysis and experimental applications. Bruckenstein and Miller (1) and Smyrl and Newman (4) have performed experiments with ring-disks to assess the nonuniform current distribution on a disk electrode utilizing the sectioned-electrode approach. Miller and Bellavance (2) have reported a number of experiments with the system, including measurement of interrupter and steady-state resistances and interactive resistances between the ring and the disk. Smyrl and Newman (3,4) have presented data for ring-disk electrodes operated at and below the limiting current, along with a detailed analysis demonstrating the limiting current calculations. The primary current distribution was recently computed by Miksis and Newman (5). The limiting current (4,11) and the primary current (5) densities of a ring electrode are not uniform, so the current density on a ring operated at some fraction of the limiting current, where kinetics also must be taken into account, does not approach the uniform distribution (12) that prevails near the edge of a disk electrode as the fraction of the limiting current approaches unity. The current distribution across a ring-disk electrode tends to be more nonuniform than for an equivalent disk.

Newman's (6) approach to the computation of the concentration and current density distributions across a rotating disk electrode has been applied successfully to a number of other electrode geometries (7,8,9,24,25). Parrish and Newman (8) investigated the current distributions on two plane parallel electrodes in channel flow, the only application to two interactive working electrodes. The ring-disk geometry contains two working electrodes and can utilize a counterelectrode, which would be considered infinitely far from the working electrodes. The working electrodes interact through the potential distribution, which is described by an elliptic Laplacian equation giving global effects, and through the parabolic concentration boundary-layer equations which allow a downstream influence on the ring electrode by the disk. The ring implicitly affects the disk concentration profile by modifying the potential which enters into the kinetic expressions, thus changing the flux boundary conditions that would exist on the disk from the situation prevailing if no ring were present.

Current can flow between any of the three electrodes in the cell, but common experimental objectives usually attempt to limit the possibilities. The ring and the disk can be operated potentiostatically with the current from each electrode being collected by the counterelectrode. The disk can be used to produce a species not in the bulk solution which can then be collected by the ring electrode, usually one electrode being driven cathodically and the other anodically. The disk electrode can be driven as a bipolar electrode

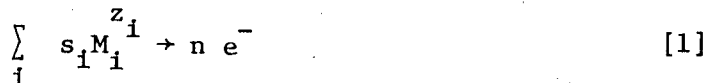
where a current loop exists in the solution over the electrode. The analysis presented here applies to all these cases, but the results are restricted to the sectioned disk, with the ring and the disk maintained at the same potential. Results for the other situations will be reported in a subsequent paper.

The kinetics of the surface reaction to be considered are of three types, a product-independent metal deposition from a single salt solution (6), a product-independent reaction with a supporting electrolyte (6), and a reaction depending on all reacting species with a supporting electrolyte (10). These reactions are representative of plating from a solution with and without a supporting electrolyte, and of redox reactions or organic synthesis with a supporting electrolyte. The analysis is restricted to laminar flows, high Schmidt numbers, and dilute solutions with constant physical properties.

The method of computing current densities and concentration profiles is developed for a ring-disk system operated potentiostatically. Integral measures of the way in which these profiles deviate from the limiting current and primary current distributions are discussed. The design of ring-disk electrodes for the purpose of measuring the throwing power is shown.

Overpotentials

For a single electrode reaction which can be expressed by



where s_i is the stoichiometric coefficient, M_i is the symbol for the chemical species, z_i is the species charge number, and n is the number of electrons participating in the reaction. The potential applied between each of the working electrodes and a single counter-electrode located at infinity is

$$V_d = U + \phi_{o,d} + \eta_c + \eta_s \quad [2]$$

$$V_r = U + \phi_{o,r} + \eta_c + \eta_s .$$

The applied potentials are separated into the equilibrium potential U which is associated with the reaction Eq. [1], a concentration overpotential η_c , a surface overpotential η_s , and an ohmic potential ϕ_o for each working electrode which is extrapolated to the surface of the electrode. The expression for the concentration overpotential (13) is

$$\eta_c = - \frac{RT}{ZF} \left[\sum_i s_i \ln \left(\frac{c_{1,\infty}}{c_{1,o}} \right) - t \left(1 - \frac{c_{1,0}}{c_{1,o}} \right) \right] . \quad [4]$$

Eq. [4] applies approximately to metal deposition from a single salt where t is the transference number of the metal ion, species 1. Z is then equal to $-z_- z_+ / (z_+ - z_-)$. For the case in which the reactants and products are minor components in a solution containing an excess of supporting electrolyte, t is zero, and Z is equal to $-n$. The surface overpotential can be related to the current density by

$$i = i_o \left[\exp \left(\frac{\alpha Z F}{RT} \eta_s \right) - \exp \left(\frac{-\beta Z F}{RT} \eta_s \right) \right] . \quad [5]$$

The kinetic parameters α and β are determined by the reaction taking place. The local exchange current density i_o is taken to have a composition dependence given by

$$i_o = i_{o,\infty} \prod_i \left(\frac{c_{i,o}}{c_{i,\infty}} \right)^{\gamma_i} . \quad [6]$$

The γ_i are specified by the particular reaction taking place and the condition of the surface upon which the reaction occurs, and $i_{o,\infty}$ is an exchange current density evaluated at the composition of the bulk solution.

Potential Distribution

The potential variation in the region of constant concentration is described by a solution of Laplace's equation which matches the current at the surface of the electrode with the mass flux through the boundary layer for a faradaic process. The particular solution found to be most suited for the ring-disk configuration operated below the limiting current is (14)

$$\phi_o(r) = \int_0^{r_2} \frac{i(r')}{r+r'} \kappa \left(\frac{4rr'}{(r+r')^2} \right) r' dr' . \quad [7]$$

The integral is evaluated at all points r' on the electrode surface where there is a nonzero value of the normal component of the current

density i , K is the complete elliptic integral of the first kind (15), and r is the radial position on the surface at which ϕ_0 is desired. The behavior of the elliptic integral K when r is equal to r' requires special care in the numerical evaluation of Eq. [7]. The integral technique for the ring-disk system when mass transfer and kinetic effects must be considered offers real computational advantages over previously used series solutions (6) and a combination of series and integrals (5).

Concentration Profile

The Lighthill transformation has been successfully applied to the problem of evaluating the concentration profile through the diffusion boundary layer in previous examples of the calculation of current distributions below the limiting current (4,7,8,9,10,24,25). The flux at the electrode surface can be expressed by (4)

$$\frac{\partial c_{i,0}}{\partial \zeta} = \frac{-r}{\Gamma(4/3)} \int_0^r \frac{dc_{i,0}}{dr'} \frac{dr'}{(r^3 - r'^3)^{1/3}} \quad [8]$$

and inverted to give

$$c_{i,0} - c_{i,\infty} = \frac{-1}{\Gamma(4/3)} \int_0^r \frac{\partial c_{i,0}}{\partial \zeta} \bigg|_{r=r'} \frac{r' dr'}{(r^3 - r'^3)^{2/3}} \quad [9]$$

Eq. [8] is equated to a flux specified by Eq. [2] or [3] and Eqs. [4] and [5] and then solved for the concentration at the electrode surface.

Eq. [9] is used to track the surface concentration variation across the insulating annulus. Eq. [9] can also be manipulated to yield

$$\frac{c_{i,0} - c_{i,\infty}}{c_{j,0} - c_{j,\infty}} = \frac{s_i}{s_j} \left(\frac{D_j}{D_i} \right)^{2/3} \quad [10]$$

One species can now be chosen and conveniently designated to be subscripted as i equal to 1, then Eq. [8] need be solved for only the value of $c_{1,0}$. All other surface concentrations needed in the expression of the electrode kinetics may be computed by Eq. [10] as long as the only reaction occurring is Eq. [1].

The total current or mass transfer rate to the electrode is a quantity which must be computed as accurately as possible if a good comparison with experimentally measured currents is desired. The ratio of the ring current to the disk current is very sensitive to errors in computing the integral values. A quantity j , proportional to the total flow of a species to the electrode surface between the limits of integration, 0 and R , is

$$j = \int_0^R \frac{\partial c_{i,0}}{\partial \zeta} r \, dr \quad [11]$$

which becomes upon substitution of Eq. [8] and one integration

$$j = \frac{-1}{2\Gamma(4/3)} \int_0^R \frac{dc_{i,0}}{dr} (R^3 - r^3)^{2/3} dr \quad [12]$$

Eqs. [8] and [12] are Stieltjes integrals, so the points at the center of the disk and the leading edge of the ring must be taken into account when evaluating the integrals. Eq. [12] can be easily solved by using the method of Acrivos and Chambre (19) utilizing the same mesh points that are generated in the solution of Eq. [8].

Numerical Solution

A set of equations are now established which can be solved numerically by the same techniques given in previous work (6,8,9,10).

The parameters that the solution depends upon are α , β , γ_1 , t ,

$\frac{r_0}{r_1}$, $\frac{r_1}{r_2}$, Z , and

$$N = - (4/3) \frac{nFr_2 i_{LIM,DISK}}{RTk_\infty} \quad [13]$$

and

$$J = \frac{i_{o,\infty} r_2 nF}{RTk_\infty} \quad [14]$$

and

$$\delta = |i_{avg}| \frac{r_2 nF}{RTk_\infty} \quad [15]$$

N is referred to species 1 so $i_{LIM,DISK}$ is the limiting current density on a disk electrode for species 1. There is a δ for both

the ring and the disk, with the appropriate average current density being substituted in Eq. [15]. J represents a dimensionless exchange current density.

Measures of Nonuniform Current Distributions

The problem of assessing the effect of nonuniform ohmic potential drop on arbitrarily shaped electrodes has long been of interest to electroplaters. A specific solution which will deposit an even thickness of metal over a range of current densities has been the goal of many experimental investigations, and is the basis of a portion of the plating industry. Haring and Blum (16) introduced the concept of defining throwing power by a well chosen experiment. Parallel, rectangular electrodes of equal area were connected by a solution contained within insulating planes normal to the electrode surfaces, which would give a uniform primary current on the electrodes and an easily defined primary resistance. Two cells with a primary current ratio of 5 were polarized with the same voltage, and currents were measured. The throwing power can then be computed by applying (16)

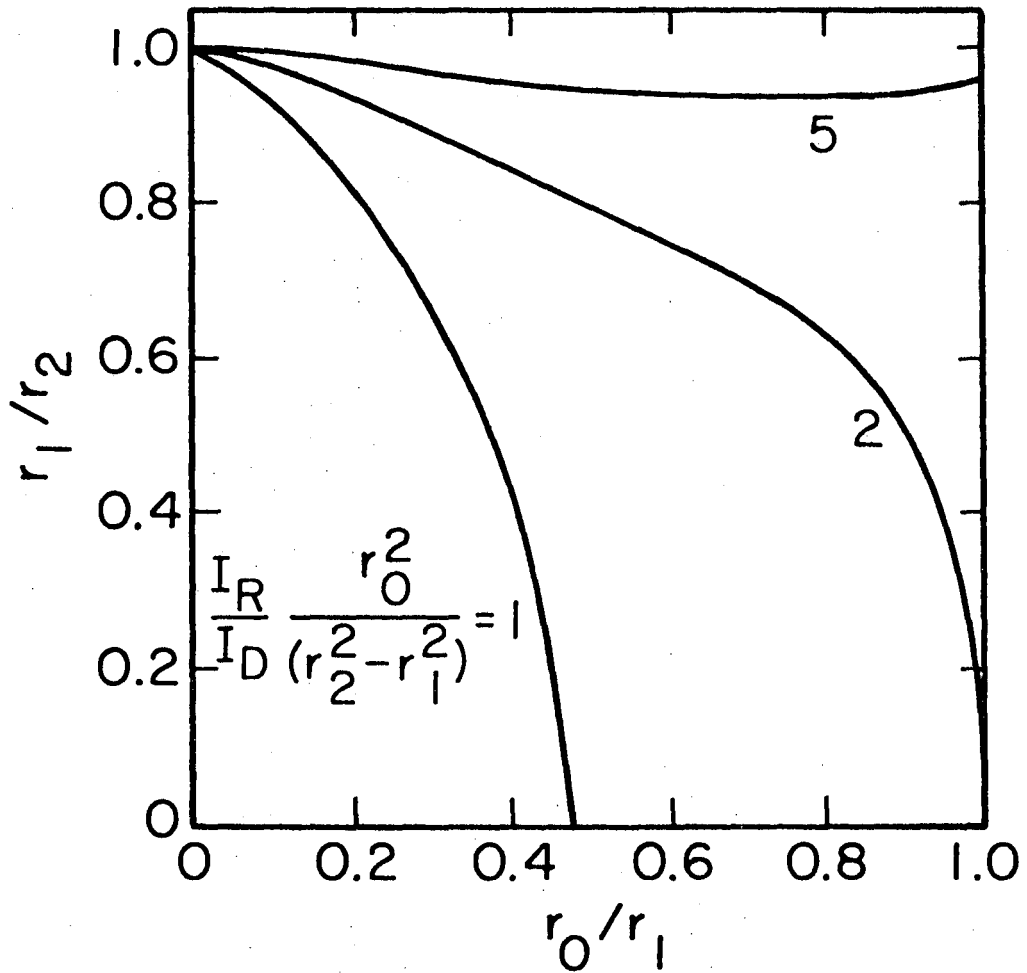
$$\text{T.P.} = \frac{\frac{I_{P1}}{I_{P2}} - \frac{I_1}{I_2}}{\frac{I_{P1}}{I_{P2}} + \frac{I_1}{I_2} - 2 \frac{A_1}{A_2}} \times 100 \quad [16]$$

I_1 and I_2 are the measured currents, I_{P1} and I_{P2} are the primary currents, and A_1 and A_2 are the areas of the electrodes. This

measurement does not characterize the solution independently of the measuring device. In an unstirred cell, natural convection becomes a significant factor as the current densities are increased. Throwing powers measured with cells having the same electrode spacing ratio but different electrode areas are usually different. The effect of natural convection can be minimized by stirring the cells, but the effect of the stirring rates must then be assessed. Studies on membranes (18) have shown that stirring can totally obscure the measurement of desired membranes properties at a surface in a well stirred tank. Thus it seems difficult at best to describe theoretically the Haring-Blum cell well enough to measure a throwing power that could be related to solution properties only.

The throwing power is a measurement of the deviation of a current ratio from the primary current ratio on two electrodes with different geometries. A rotating ring-disk electrode system is a good device to make this type of measurement since the primary current distribution is now known (5), and the effects of stirring are well characterized by N. Fig. 1 shows the radius ratios necessary to construct a ring-disk electrode with a given average primary current density ratio. The average current density ratio must be used instead of the current ratio as in the Haring-Blum cell because the electrode areas are not equal. Throwing powers for ring-disk systems can be computed as a function of the device parameters and solution parameters by setting $V_r = V_d$.

Another measure of nonuniformity is a deviation from the limiting current distribution, which is uniform on the disk but not on the ring.



XBL 767-8575

Fig. 1. Design curves for ring-disk electrodes with a given average primary current ratio.

A useful parameter f_2 can be defined (4) as the ratio of the current to the ring, divided by the area of both the ring and the insulating gap, to the average current density on the disk

$$f_2 = \frac{I_r}{I_d} \frac{r_o^2}{r_2^2 - r_o^2} \quad [17]$$

The value of f_2 compared to the value for the limiting current distribution

$$\Delta = f_2 - f_{2,LIM} \quad [18]$$

then provides the measure of deviation from the limiting distribution.

Results and Discussion

The number of possible combinations of reaction, solution, and electrode parameters is enormous. The discussion will be restricted to two electrode geometries, two limiting cases, and the results of an experiment.

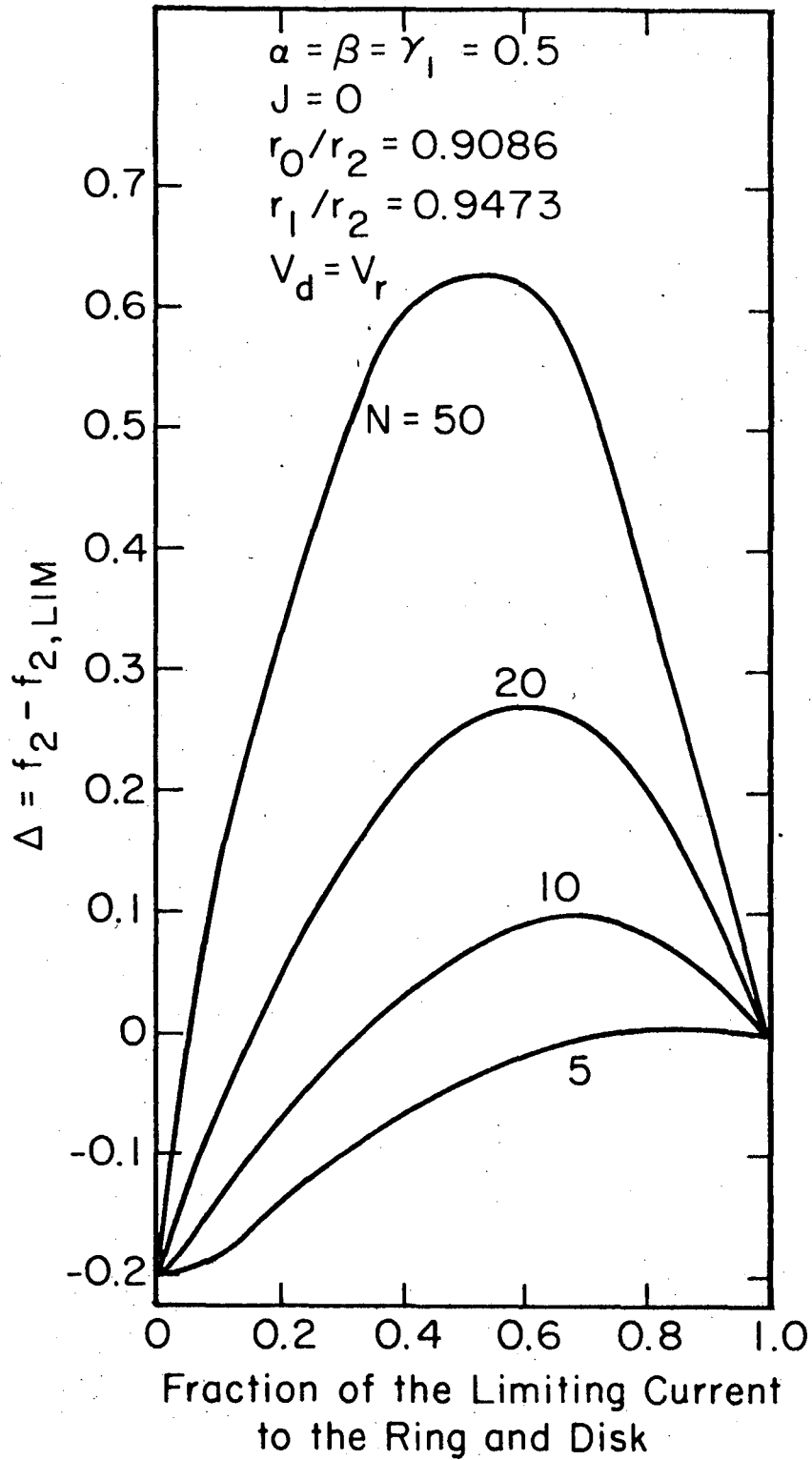
Tafel Kinetics. When $|i| \gg i_o$, one exponential term in Eq. [5] becomes negligible in comparison to the other. For cathodic current densities, Eq. [5] may then be represented by

$$\eta_s = -\frac{RT}{\beta ZF} (\ln |i| - \ln i_o) \quad [19]$$

The other term of Eq. [5] would be retained if the current were anodic.* Figure 2 shows the variations of Δ for a ring-disk operated potentiostatically, with V_d set equal to V_r . At low rotation speeds or smaller values of N , little deviation from the limiting current ratios appears until the electrodes are operating appreciably below the limiting current. However, for the higher values of N , there exist large variations in Δ over the entire operating range. At very low currents, all the curves on Fig. 2 come together at $\Delta = -0.205$. Here the Tafel kinetics force the current density to be uniform and equal on the disk and ring electrodes.

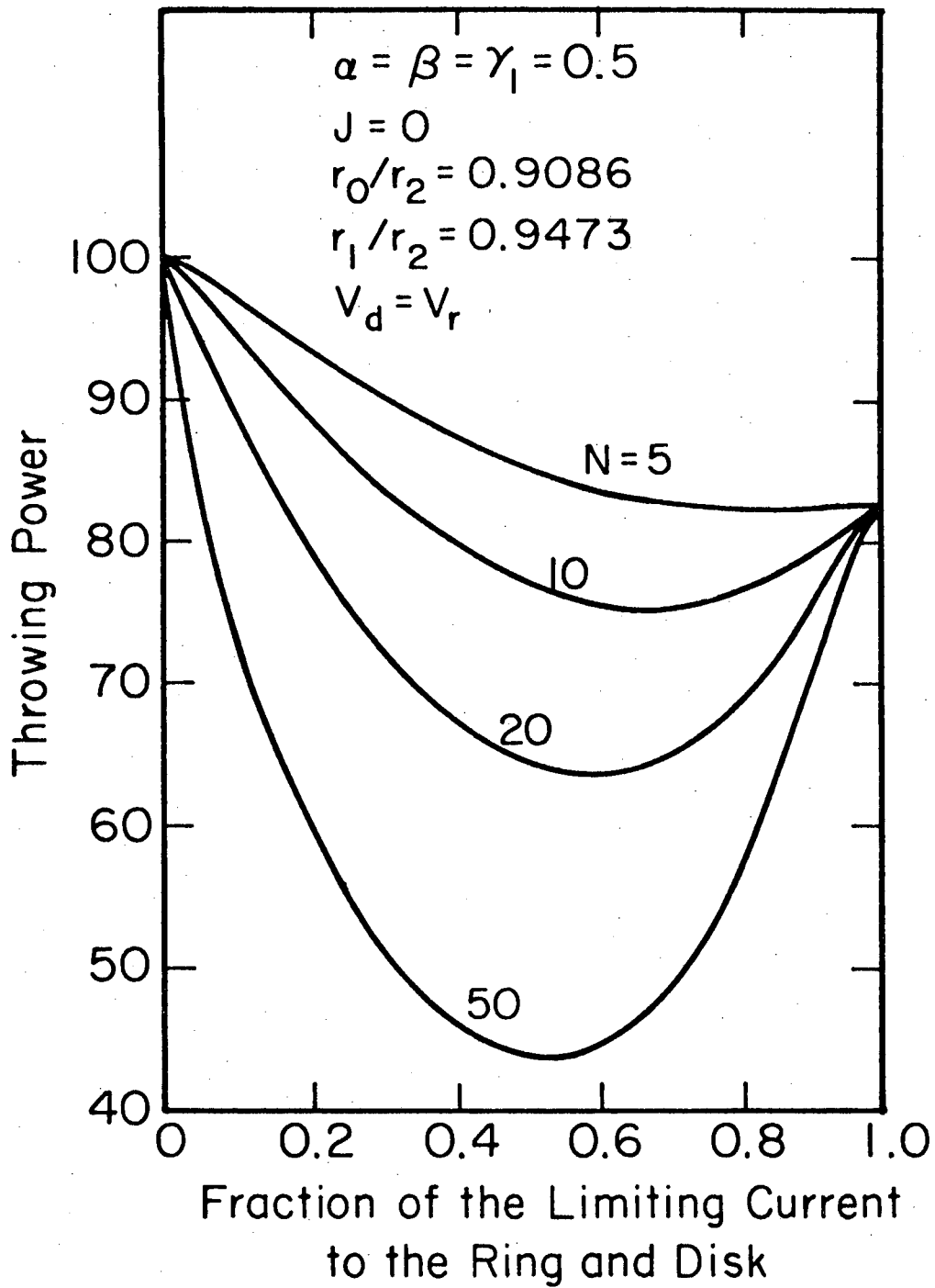
Figure 3 gives the values of the throwing power for the same electrode and solution. The effect of N is reflected in the same overall manner by Δ and by the throwing power. N becomes smaller as the electrical conductivity increases, illustrating the effect of increasing κ_∞ on the throwing power. N is proportional to r_2 and therefore gives a qualitative idea of how the characteristic dimensions of irregularly shaped objects would influence the throwing power of a given plating bath. Another interesting feature is the approximate location of the minimum in the family of throwing power curves. Limits on allowable current densities in a plating situation would be placed on either side of this point to minimize the variation of deposit thickness.

* Z will be negative for reduction of an anion or oxidation of a cation. In such a case, the words anodic and cathodic should be interchanged in the text.



XBL 768-10152

Fig. 2. The variation of Δ calculated for metal deposition from a solution with supporting electrolyte for Tafel kinetics and several stirring rates.

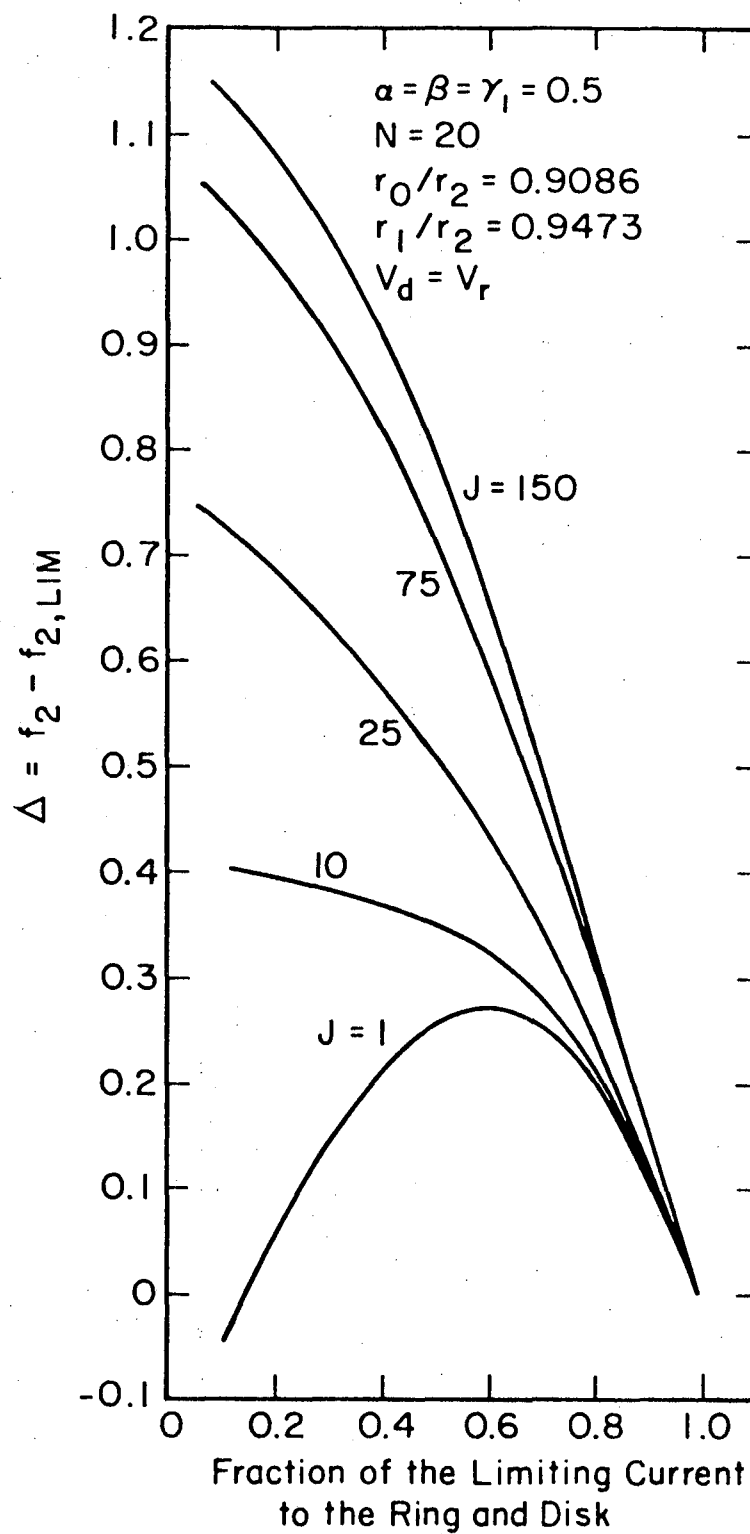


XBL 768-10155

Fig. 3. The variation of the throwing power calculated for metal deposition from a solution with supporting electrolyte for Tafel kinetics and several stirring rates.

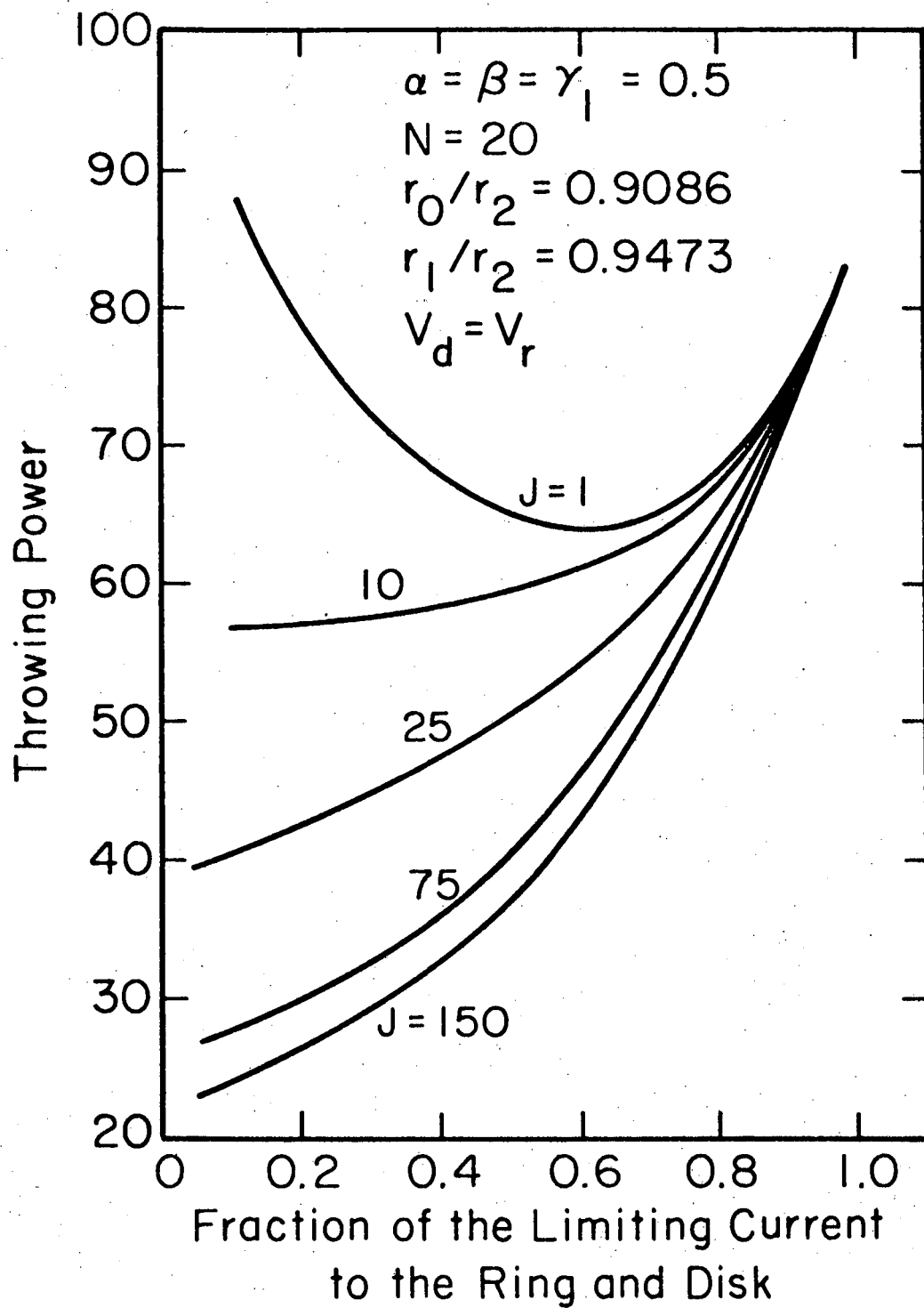
Intermediate Kinetics. The situation in which no single aspect of the concentration or surface overpotential expressions is dominant may be termed intermediate kinetics. For the same electrode used to demonstrate Tafel kinetics, a moderate dimensionless stirring rate N was chosen, and five values of the dimensionless exchange current density J were used to show the effect of concentration and surface overpotential on Δ in Fig. 4 and the throwing power in Fig. 5. When J is small and the reaction is considered slow, the current distribution is quite uniform for small fractions of the limiting current. This corresponds to $\Delta = -0.205$ for this geometry. For larger values of J , the surface overpotential becomes less important. The current distribution would approach a primary distribution for smaller values of the average current (and high rotation speeds). This corresponds to $\Delta = 1.977$ and a throwing power of zero for this geometry. The behavior at high average currents is determined more by the effect of mass transfer, and the influence of kinetic parameters decreases.

Comparison with Experiment. The smooth curve in Fig. 6 is the computed variation of Δ for curve A of Fig. 1 in the work of Smryl and Newman (4), and the points are experimentally determined (20). The values of α , β , γ_1 , and γ_2 are taken from the literature (21) for the ferri-cyanide-ferrocyanide redox couple. The value of the exchange current density used to compute J was estimated with Eq. 6 from the experimentally determined value reported by Vetter (22). The conductivity of the bulk solution was determined to be $0.0894 \text{ ohm}^{-1} \text{ cm}^{-1}$ in our laboratory, thus yielding a somewhat different value of N from that estimated earlier (4). The remaining parameters were measured (20). Good agreement between the computation and the experiment is shown.



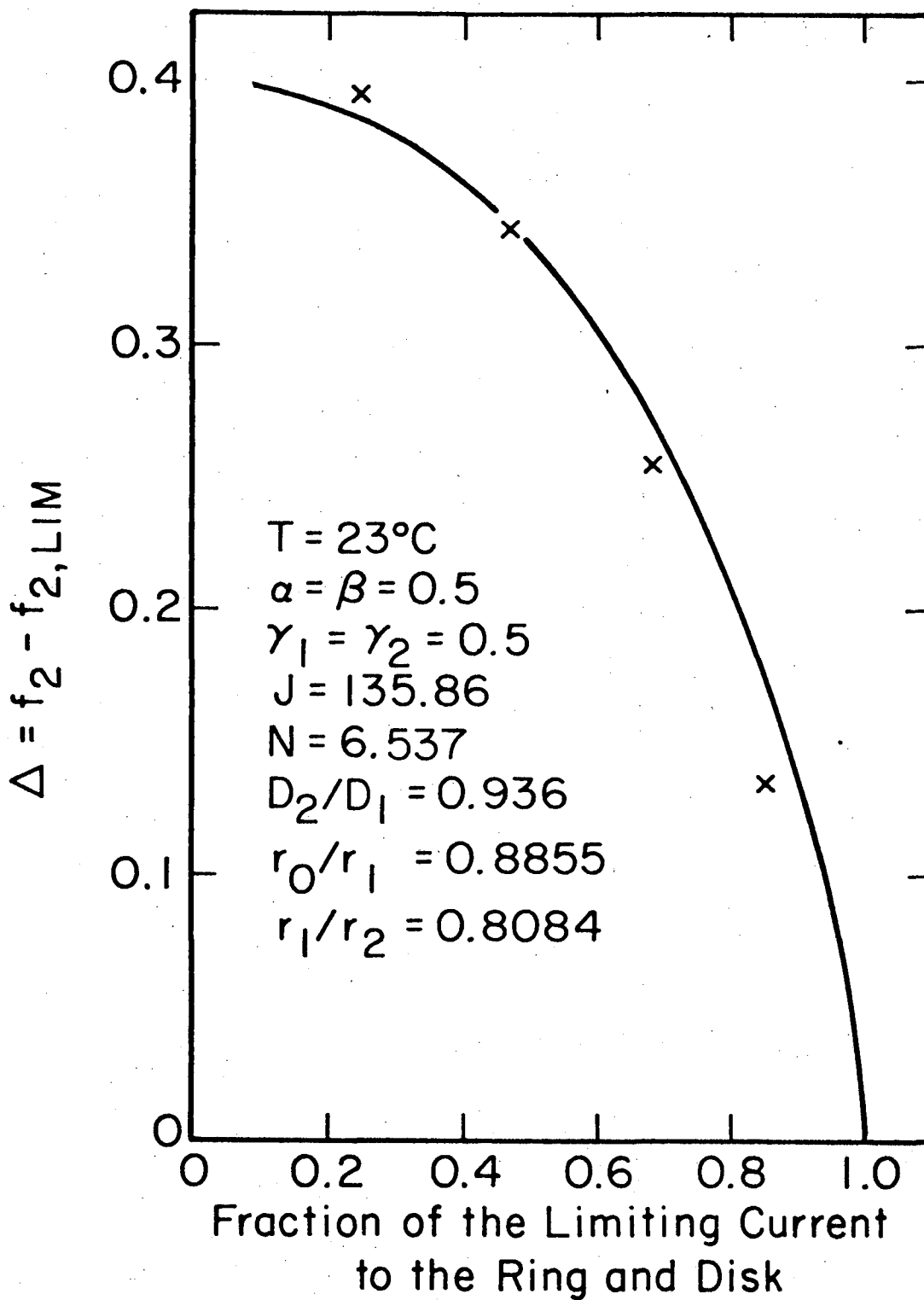
XBL 768-10153

Fig. 4. Computed values of Δ for metal deposition from a solution with supporting electrolyte for a fixed stirring rate and for five values of the dimensionless exchange current density.



XBL 768-10154

Fig. 5. Computed values of the throwing power for metal deposition from a solution with supporting electrolyte for a fixed stirring rate and for five values of the dimensionless exchange current density.



XBL 768-10151

Fig. 6. Δ shown as a function of the fraction of the limiting current with $V_d = V_r$. Points are measured and the smooth curve computed for a 1 M KNO_3 , 0.05 M $\text{K}_3\text{Fe}(\text{CN})_6$, 0.05 M $\text{K}_4\text{Fe}(\text{CN})_6$ solution. Ferrocyanide is the reference species and is being oxidized at the electrodes.

Acknowledgement

This work was supported by the United States Energy Research and Development Administration.

List of Symbols

English characters

A_1, A_2	area of electrode 1 or 2, cm^2
a	0.51023
c_1	concentration of species i , mole/cm^3
$c_{i,0}$	concentration of species i at the electrode surface, mole/cm^3
$c_{i,\infty}$	concentration of the i th species in the bulk solution, mole/cm^3
D_i	diffusion coefficient of the i th species, cm^2/s
f_2	dimensionless ratio of ring to disk current densities see Eq. [17]
$f_{2,\text{LIM}}$	Eq. [17] applied to the limiting current distribution
F	Faraday's constant, 96487 C/equiv
i	normal current density at the electrode surface, A/cm^2
i_0	local exchange current density, A/cm^2
$i_{0,\infty}$	characteristic exchange current density, A/cm^2
$i_{\text{LIM},\text{DISK}}$	limiting current density for species 1 on a disk electrode, A/cm^2
I_{P1}	primary current for electrode 1, A
I_{P2}	primary current for electrode 2, A
I_1	current to electrode 1, A

I_2	current to electrode 2, A
j	proportional to the average or total mass transfer rate, mole/cm
J	dimensionless exchange current density
M_i	chemical symbol for the species i
N	dimensionless stirring rate
n	number of electrons in reaction
R	universal gas constant, 8.3143 J/mole-K
r	radial coordinate, cm
r_0	radius of disk electrode, cm
r_1	inner radius of ring electrode, cm
r_2	outer radius of ring electrode, cm
s_i	stoichiometric coefficient of i th species
t	transference number of reactant
T	absolute temperature, K
T.P.	throwing power, see Eq. [16]
U	open circuit potential, V
V_d	potential applied between the disk and the counter- electrode, V
V_r	potential applied between the ring and the counter- electrode, V
y	normal distance from the surface, cm
z_i	charge number of i th species
Z	$-n$ or $-z_+z_-/(z_+ - z_-)$

Greek characters

α, β	parameter, in Eq. [5]
γ_i	parameters in Eq. [16]
δ	dimensionless average current density
Δ	dimensionless deviation of f_2 from limiting current f_2 , see Eq. [18]
ζ	dimensionless normal distance from surface, $y(a\nu/3 D_i)^{1/3} (\Omega/\nu)^{1/2}$
η_c	concentration overpotential, V
η_s	surface overpotential, V
κ^∞	electrical conductivity of the bulk solution, $\text{ohm}^{-1}\text{-cm}^{-1}$
ν	kinematic viscosity
Φ_0	potential extrapolated to the surface, V
Ω	rotation speed, rad/s.

Reference

1. S. Bruckenstein and B. Miller, This Journal, 117, 1044 (1970).
2. B. Miller and M. I. Bellavance, ibid., 120, 42 (1973).
3. W. H. Smryl and J. Newman, ibid., 119, 208 (1972).
4. W. H. Smryl and J. Newman, ibid., 119, 212 (1972).
5. J. J. Miksis, Jr., and J. Newman, ibid., 123, 1030 (1976).
6. J. Newman, ibid., 113, 1235 (1966).
7. W. R. Parrish and J. Newman, ibid., 116, 169 (1969).
8. W. R. Parrish and J. Newman, ibid., 117, 43 (1970).
9. K. Nişancıoğlu and J. Newman, ibid., 121, 241 (1974).
10. P. Pierini, P. Appel, and J. Newman, ibid., 123, 366 (1976).
11. V. G. Levich, Physiochemical Hydrodynamics, Prentice-Hall, Inc., p. 107 (1962).
12. V. G. Levich, Acta Physiochim., U.R.S.S., 17, 257 (1942).
13. J. Newman, Intern. J. Heat Mass Transfer, 10, 983 (1967).
14. J. Newman, "The Fundamental Principles of Current Distribution and Mass Transport in Electrochemical Cells," A. J. Bard, ed., Electroanalytical Chemistry, 6, 326 (1973).
15. M. Abramowitz and I. A. Stegun, eds., Handbook of Mathematical Functions, National Bureau of Standards, Washington, p. 608 (1964).
16. H. E. Haring and W. Blum, Trans. Amer. Electrochem. Soc., 44, 313 (1923).
17. T. P. Hoar and J. N. Agar, Discussions of the Faraday Society, 1, 162 (1947).
18. C. K. Colton and K. A. Smith, A.I.Ch. E. Journal, 18, No. 5, 958 (1972).

19. A. Acrivos and P. L. Chambre, Ind. Eng. Chem., 49, 1025 (1957).
20. W. H. Smryl, Private communication (1975).
21. F. A. Posey and S. S. Misra, This Journal, 113, 608 (1966).
22. K. J. Vetter, Electrochemical Kinetics, Academic Press, p. 493 (1967).
23. Ch. W. Tobias and R. Hickman, Z. Phys. Chem., 229, 145 (1965).
24. R. V. Homsy and J. Newman, This Journal, 121, 1448 (1974).
25. R. Alkire and A. A. Mirarefi, ibid., 120, 1507 (1973).
26. R. Cabán and T. W. Chapman, ibid., 123, 1036 (1976).

This report was done with support from the United States Energy Research and Development Administration. Any conclusions or opinions expressed in this report represent solely those of the author(s) and not necessarily those of The Regents of the University of California, the Lawrence Berkeley Laboratory or the United States Energy Research and Development Administration.

TECHNICAL INFORMATION DIVISION
LAWRENCE BERKELEY LABORATORY
UNIVERSITY OF CALIFORNIA
BERKELEY, CALIFORNIA 94720